

# Theodorsen's Ideal Propeller Performance with Ambient Pressure in the Slipstream

Gerrit Schouten\*  
Delft University of Technology,  
2629 HS Delft, The Netherlands

## I. Introduction

THEODORSEN'S propeller theory<sup>1</sup> provides a rational estimation of the highest efficiency attainable for specified operating conditions. However, the theory suffers from the deficiency that it yields a static pressure in the slipstream which is too high by an amount of  $O[\rho w^2/2]$ , where  $w$  is the relative velocity of the trailing vortex system. This high pressure explicitly is a consequence of Theodorsen's model, inspired by Betz's<sup>2</sup> rigidly moving trailing vortex sheets providing minimum induced drag. The unrealistic notion of rigidly moving trailing vortex sheets (neglecting the rolling-up of the sheets) is very useful for the kinematical computation of the ideal propeller blade loading and the associated bound vorticity distribution. For that computation it is allowed to neglect the rolling-up because the exact far-downstream shape of the sheets has only a minor influence on the induced velocities in the propeller area. When it comes to computation of the pressure in the slipstream, a more realistic model incorporating the rolling-up of the sheets as suggested by Schouten<sup>3</sup> is probably more appropriate. It must be understood that the half-infinite rigid helicoidal trailing vortex sheet system is unrealistic because it is not force-free. It could only survive as a bound system, capable of sustaining the edge forces. In reality, the sheets start rolling-up at the edges as soon as they leave the material propeller blade and become free-trailing sheets. As a consequence of the high pressure in the slipstream, Theodorsen's theory leads to the optimistic result that the required power is less than what one would roughly expect from the product of thrust  $T$  and axial velocity  $(V + w/2)$  at the propeller blades. (The rigid helicoidal sheets, moving rearward with  $w$  in the Trefftz-plane, are supposed to move with  $w/2$  when they are shed by the propeller). The power coefficient  $c_p$  as found by Theodorsen in Ref. 1, and re-established recently by Ribner and Foster,<sup>4</sup> is

$$c_p = 2\kappa\bar{w}(1 + \bar{w})[1 + (\epsilon/\kappa)\bar{w}] \quad (1)$$

From a rough estimation one would expect a higher power coefficient  $c_p^*$ . The product of thrust (using Theodorsen's thrust coefficient) and  $V + w/2$  would yield the value

$$c_p^* = 2\kappa\bar{w}\{1 + \bar{w}[\frac{1}{2} + (\epsilon/\kappa)]\}[1 + (\bar{w}/2)] \\ = c_p + (\bar{w}^2/2)[\frac{1}{2} - (\epsilon/\kappa)] \quad (2)$$

The difference between Theodorsen's result,  $c_p$ , and the expected minimum value  $c_p^*$ , leads for values of  $\lambda_T$  above 0.75 to an underestimation by Theodorsen, because then  $\epsilon/\kappa$  becomes smaller than 0.5.

The remedy proposed for both the deficiencies, the high pressure in the slipstream, and the low required power, is to allow the outer parts of the helicoidal sheets to roll up in helicoidal vortices wrapped around an inhomogeneous slipstream. The inner part contains the more axially directed trailing vortices mainly taking care of the rotation of the core.

Received Nov. 30, 1991; revision received April 24, 1992; accepted for publication May 22, 1992. Copyright © 1992 by the American Institute of Aeronautics and Astronautics Inc. All rights reserved.

\*Staff Member, Department of Aerospace Engineering, Kluuyverweg 1.

The rolling-up of the sheets induces the free vortices to move with a velocity  $w/2$ , this velocity being the average of the outer situation (zero velocity) and the conditions inside the slipstream where the sheets by definition moved with  $w$ . The  $\partial\Phi/\partial t$ -term, which causes the high pressure in Theodorsen's model, is halved by the reduction of the velocity of the vortices to  $w/2$ .

It is not our aim to rephrase Theodorsen's theory, only the effects on the expressions for the thrust coefficient  $c_s$ , the power coefficient  $c_p$ , and the efficiency  $\eta$  will be discussed in detail. For the theory we will refer to Theodorsen's book<sup>1</sup> and to Ribner and Foster's paper.<sup>4</sup> Ribner and Foster do not comment on the theory, they present a computer algorithm for the computation of the ideal blade circulation  $K(r/R)$  and the key parameters  $\kappa$  and  $\epsilon/\kappa$  derived from it. Furthermore, they present the results in a convenient format, due to Kramer.<sup>5</sup> It is these results, plots of power coefficient vs advance ratio at constant efficiency that are affected by the modification presented below. The general properties of the potential flow model, i.e.,  $K(r/R)$  and the parameters  $\kappa$  and  $\epsilon/\kappa$ , remain as they are and we used them as presented in Figs. 1 and 2 of Ribner and Foster.<sup>4</sup> Sticking to these values of  $\kappa$  and  $\epsilon$  implies that the axial mass transport,  $\kappa\rho wA$ , and the axial momentum transport,  $\epsilon\rho w^2A$ , are supposed to be unaffected by the rolling-up of the sheets. Neither the exact diameter of the vortex-spirals nor the cross-sectional area of the vortices need to be further specified. In the model their values are supposed to settle such as to ensure conservation of mass and momentum.

## II. Momentum and Energy Theorems

Applying Newton's law (the momentum balance) to a large volume  $C$  (see Fig. 1) around the propeller we have

$$\text{total force } \bar{F} = \frac{D}{Dt} \int_{C(t)} \int \rho \bar{v} dV \quad (3)$$

Using Reynolds' transport theorem<sup>6</sup> and rearranging terms we get the integral [Eq. (4)] for the propeller thrust  $T$

$$T + \int \int (p_0 - p_s) dS = \rho \int \int (V + v_z) v_z dS \quad (4)$$

[note that the  $T$  in Eq. (4) is a force on the air in the positive  $z$  direction, the thrust on the propeller is  $T$ , positive in the negative  $z$  direction]. The pressure  $p_s$  is found from the unsteady Bernoulli Eq. (5):

$$p = p_0 - \rho v^2/2 - \rho \partial\Phi/\partial t \quad (5)$$

It is the  $\partial\Phi/\partial t$  term that causes the high pressure in Theodorsen's formulation. Considering the helicoidal vortex sheet system to move rigidly backwards with  $w$  (as Theodorsen does), we have  $\Phi = \Phi(z-wt, r, \theta)$  and  $\rho \partial\Phi/\partial t = -\rho \partial\Phi/\partial z w = -\rho v_z w$ . When we consider the sheets to be rolled-up, the resulting vortices move with  $w/2$  and we have  $\Phi = \Phi(z-wt/2, r, \theta)$ , leading to  $\rho \partial\Phi/\partial t = -\rho \partial\Phi/\partial z (w/2) = -\rho v_z (w/2)$ .

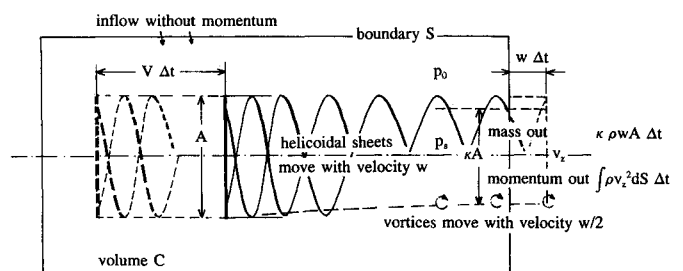


Fig. 1 Control volume  $C$  around a propeller moving with  $V$  in an atmosphere at rest.

In the following, we present the formulas of Theodorsen (with index  $T$ ) and the formulas as they result from the proposed modification next to each other. The thrust would yield

$$\begin{aligned} T_T &= \rho \int \left[ (V + v_z)v_z + v_z w - \frac{v^2}{2} \right] dS \\ T &= \rho \int \left[ (V + v_z)v_z + v_z \frac{w}{2} - \frac{v^2}{2} \right] dS \end{aligned} \quad (6)$$

Note that  $w$  only enters through  $\partial\Phi/\partial t$ , we left  $v_z$  to be the distributed axial velocity. We find the power delivered by the propeller by applying the energy balance to the control volume, the general expression is

$$P = TV + \int \left[ (p_s - p_0)v_z + \rho(V + v_z) \frac{v^2}{2} \right] dS \quad (7)$$

leading to the different expressions for  $P_T$  and  $P$

$$\begin{aligned} P_T &= T_TV + \rho \int \left( v_z^2 w + V \frac{v^2}{2} \right) dS \\ &= \rho \int (Vv_z + v_z^2)(V + w) dS \\ P &= TV + \rho \int \left( v_z^2 \frac{w}{2} + V \frac{v^2}{2} \right) dS \\ &= \rho \int (Vv_z + v_z^2) \left( V + \frac{w}{2} \right) dS \end{aligned} \quad (8)$$

The integrals involving  $v$  and  $v_z$  are evaluated in the potential flow model. Theodorsen<sup>1</sup> used an electrical analogon to arrive at the value of the integrals, Ribner and Foster<sup>4</sup> use a computational method. We will use the same definitions [Eq. (9)] as Theodorsen for the nondimensional parameters  $\kappa$  and  $\varepsilon$ ,  $\kappa$  is the mass factor and  $\varepsilon$  is the axial loss factor (also quantifying the axial momentum transport

$$\kappa \equiv \int \int \frac{v_z dS}{wA} = \int \int \frac{v^2 dS}{w^2 A}; \quad \varepsilon \equiv \int \int \frac{v_z^2 dS}{w^2 A} \quad (9)$$

That the integral involving  $v^2 dS$  leads to the value  $\kappa$  has been shown by Theodorsen.<sup>1</sup> The values of  $\kappa$  and  $\varepsilon$  are computed by Ribner and Foster<sup>4</sup> and presented as a function of  $\lambda_T = (V + w)/(\pi nD) = \lambda(1 + w/V)$  and the number of blades  $B$ . Defining the thrust and power coefficients as

$$c_s = 2T/(\rho V^2 A); \quad c_p = 2P/(\rho V^3 A) \quad (10)$$

we arrive at Eq. (11), where we introduced the notation  $w/V = \bar{w}$

$$\begin{aligned} (c_s)_T &= 2\kappa\bar{w}[1 + \bar{w}(\frac{1}{2} + \varepsilon/\kappa)]; \quad c_s = 2\kappa\bar{w}[1 + (\varepsilon/\kappa)\bar{w}] \\ (c_p)_T &= 2\kappa\bar{w}(1 + \bar{w})[1 + (\varepsilon/\kappa)\bar{w}] \\ c_p &= 2\kappa\bar{w}[1 + (\bar{w}/2)][1 + (\varepsilon/\kappa)\bar{w}] \end{aligned} \quad (11)$$

As a consequence of these expressions the efficiency  $\eta_T$  and the improved efficiency  $\eta$  get the form

$$\begin{aligned} \eta_T &= \frac{(c_s)_T}{(c_p)_T} = \frac{1 + \bar{w}(\frac{1}{2} + \varepsilon/\kappa)}{(1 + \bar{w})(1 + \bar{w}\varepsilon/\kappa)} \\ \eta &= \frac{c_s}{c_p} = \frac{1}{1 + \bar{w}/2} \end{aligned} \quad (12)$$

It seems unrealistic at first sight that the expression for  $\eta$  in terms of  $w/V$  becomes identical to the one for the actuator surface; one must note, however, that the  $w$  of the vortex

sheets in the slipstream of a propeller is higher than the  $w$  in the homogeneous slipstream of an actuator surface yielding the same thrust.

Note that for an actuator surface  $v = v_z = w$ , so that in case  $\varepsilon = \kappa$ , the value of  $\kappa$  then is  $\kappa = (V + w/2)/(V + w)$ .

### III. Results and Conclusions

Diagrams of power coefficient at constant efficiency vs advance coefficient  $\lambda = V/\pi nD$  for propellers with  $B = 2$  blades are presented by Ribner and Foster in their Figs. 5 of Ref. 4. Following Kramer,<sup>5</sup> the same diagrams apply with shifted scale to  $B = 3, 4, 5, 6, 8, 10, 12$ , or  $\infty$ . The modification of the model as proposed in this note severely affects these diagrams. Making use of the values of  $\kappa$  and  $\varepsilon/\kappa$ , as computed by Ribner and Foster we computed the thrust and power coefficients as they would result from the proposed modified theory. In Fig. 2 a number of modified curves are plotted as fat lines together with the curves of Ribner and Foster.

Diagrams of ideal  $\eta$  vs  $c_p$  for various blade numbers  $B$  at constant advance coefficient  $\lambda = 1$  are presented by Ribner and Foster in their Fig. 6 of Ref. 3. This ideal efficiency is also reduced by the proposed modification.

The modified lines for  $B = 2$  and for  $B = \infty$  are plotted as fat lines in the graph of Ribner and Foster as shown in Fig. 3.

As a conclusion, we state that the changes evoked by the proposed modification are substantial. The deficiencies of the rigid sheet model, i.e., high static pressure in the wake and underestimated required power, are both cured and the model is more in agreement with physical reality. The results should therefore be incorporated in a revised "theory of propellers."

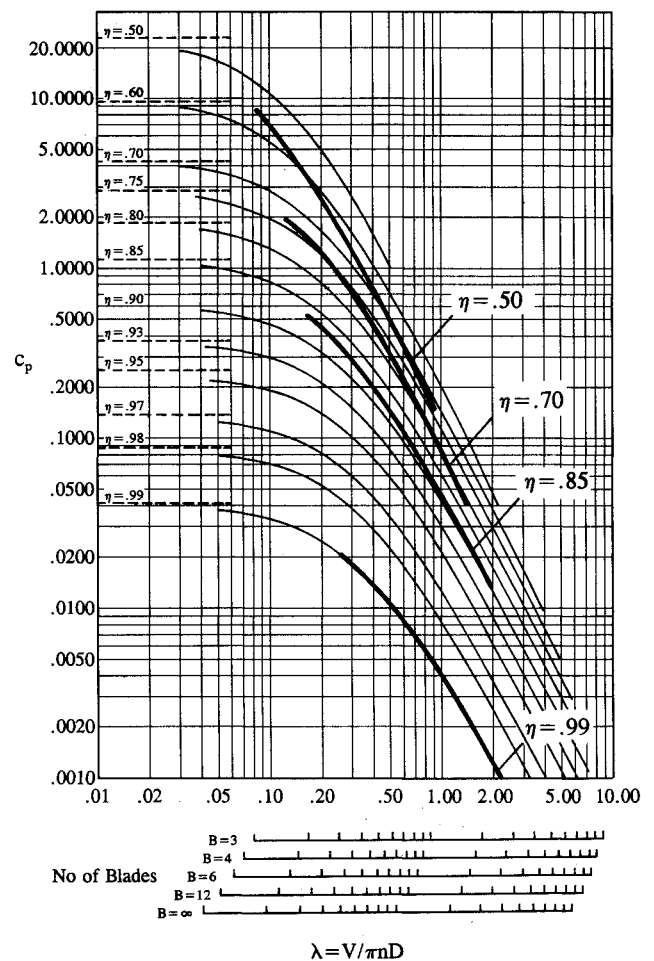


Fig. 2  $c_p$  at constant  $\eta$ .

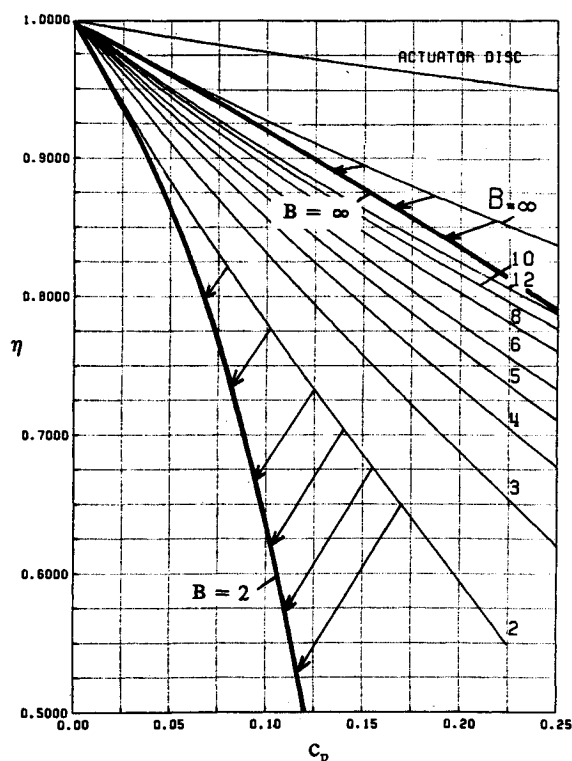


Fig. 3 Ideal  $\eta$  vs  $c_p$  at  $\lambda = 1$ ; various numbers of blades  $B$ .

### References

- <sup>1</sup>Theodorsen, T., *Theory of Propellers*, McGraw-Hill, New York, 1948.
- <sup>2</sup>Betz, A., "Schraubenpropeller mit geringsten Energieverlust," *Mitt. Nachr. d. Kgl. Ges. d. Wiss. zu Göttingen. Math. Phys. Klasse*, Heft 2, 1919; see also Prandtl, L., Appendix to Ref. 2.
- <sup>3</sup>Schouten, G., "Static Pressure in the Slipstream of a Propeller," *Journal of Aircraft*, Vol. 19, No. 3, 1982, pp. 251, 252.
- <sup>4</sup>Ribner, H. S., and Foster, S. P., "Ideal Efficiency of Propellers: Theodorsen Revisited," *Journal of Aircraft*, Vol. 27, No. 9, pp. 810–819.
- <sup>5</sup>Kramer, K. N., "The Induced Efficiency of Optimum Propellers Having a Finite Number of Blades," *Luftfahrtforschung*, Vol. 15, 1938, pp. 326–333; see also NACA TM 884.
- <sup>6</sup>Aris, R., *Vectors, Tensors, and the Basic Equations of Fluid Mechanics*, Prentice-Hall, Englewood Cliffs, NJ, 1962, pp. 84–85.

## Permeable Airfoils in Incompressible Flow

Virgil M. Musat\*

*Institute of Applied Mathematics of the Romanian Academy, Bucharest, Romania*

### Nomenclature

- $C_L$  = lift coefficient  
 $c$  = chord of airfoil  
 $c_p$  = pressure coefficient

- $c_{pc}$  = pressure coefficient in cavity  
 $M$  = freestream Mach number  
 $p$  = porosity  
 $Re$  = Reynolds number  
 $s$  = length of permeable region  
 $V$  = total velocity  
 $x, z$  = Cartesian coordinates  
 $\alpha$  = incidence angle

### Introduction

THE improvement of aircraft's handling in stall and the increasing of lift are two major aims in aircraft design. A possibility of attaining these seems to be with the use of airfoils with a permeable region, which work like self-adapting airfoils.

The idea of utilizing permeable regions for diminishing the pressure gradient through shock waves on airfoils in transonic flows was initiated by Savu and Trifu.<sup>1</sup> Great pressure gradients also appear at high incidences and, therefore, it seems reasonable to use permeable regions in incompressible flows.

Real flows over airfoils, especially at high incidences, represent an adaptation of the potential flow to the special conditions induced by viscosity. Attached flow regions are in the neighborhood of separated flow regions, like that of long bubbles. The basic idea in this note is to use, from the real flow, the effects of bubbles to improve the performances of the airfoils, especially at high incidences. In this manner, self-adaptive airfoils can be obtained, with lift close to that in potential flow.

The interaction between the external and internal flow in an unventilated cavity (see Fig. 1) through a permeable boundary, give rise to a "provoked bubble." The form and height of this bubble is the function of the external pressure and the permeability function  $p$ . In the potential model, the provoked bubble has three functions: 1) the diminution of leading edge peak, 2) the diminution of positive pressure gradient after peak, and 3) the increase of airfoil lift. In other words, the role of the provoked bubble is to smooth the pressure distribution. It is expected that all these functions could enhance the boundary-layer capability and therefore improve the behavior of the airfoil near stall.

### Analysis

A zonal solution method (Fig. 1) was adopted. For the secondary flow in a cavity and bubble, and for the principal inviscid flow around the airfoil, a potential model was considered. For the viscous flow on the airfoil and the bubble boundary it was considered the boundary-layer model.

A secondary self-adapting flow forms, in the leading-edge (i.e.) region, because of the pressure gradient through the permeable region. This flow is subject to the Darcy law

$$V_n = p(c_p - c_{pc}) \quad (1)$$

which states that the normal velocity  $V_n$ , on a permeable surface is proportional to the pressure gradient between its

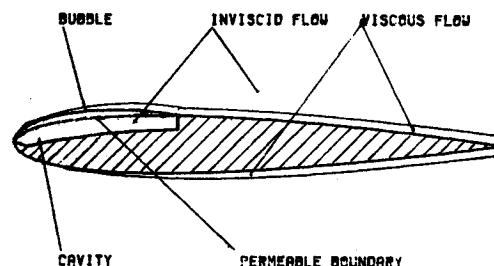


Fig. 1 Permeable airfoil.